Desalination and Water Treatment
www.deswater.com
doi: 10.5004/dwt.2019.24343

162 (2019) 391–398
September

Fenton-based processes for the regeneration of biochar from *Syagrus coronata* biomass used as dye adsorbent

Renata Silva de Lima[a], Carmem Lúcia de Paiva e Silva Zanta[a,*], Lucas Meili[b], Pollyanna Vanessa dos Santos Lins[b], Grazielle Emanuella de Souza dos Santos[b], Josealdo Tonholo[a]

[a]*Institute of Chemistry and Biotechnology, Federal University of Alagoas, 57072-900 Maceió AL, Brazil, emails: clp@qui.ufal.br (C.L. de Paiva e Silva Zanta), renat_sl@hotmail.com (R.S. de Lima), tonholo@gmail.com (J. Tonholo)*
[b]*Laboratory of Processes, Center of Technology, Federal University of Alagoas, 57072-900 Maceió AL, Brazil, emails: lucas.meili@ctec.ufal.br (L. Meili), polly_lins91@hotmail.com (P.V. dos Santos Lins), grazi.gess@hotmail.com (G.E. de Souza dos Santos)*

Received 10 November 2018; Accepted 26 April 2019

ABSTRACT

The present work aims to evaluate the application of Fenton reaction as a method for the adsorbent regeneration. The adsorbent was obtained by the thermal decomposition of *Syagrus coronata* endocarp under vacuum at relatively low temperatures (i.e., 400°C and 800°C). The biochar capacity of methylene blue removal was evaluated in function of time of contact, particle diameter and pyrolysis temperature. The biochar was characterized by X-ray diffraction and thermogravimetric analysis techniques. The highest adsorption capacity was 99.4%, obtained for 4.8 g of adsorbent, pyrolysis at 800°C and particle diameter <0.149 mm. The data obtained from the kinetic studies fitted better to the pseudo-second-order model, while the adsorption isotherms followed Sips model. Fenton regeneration was conducted using a dye saturated biochar with Fenton reagents at different concentrations of Fe^{2+} (0.5–1.0 mmol L^{-1}) and H_2O_2 (100–2,400 mmol L^{-1}) in pH = 3.0 for 30 min. A maximum recovery of 19.31% of the adsorption capacity was obtained using Fenton with Fe^{2+} 1.0 mmol L^1 and H_2O_2 600 mmol L^{-1}. Therefore, results showed that the biochar of *Syagrus coronata* endocarp was effective to remove methylene blue from water solution and Fenton reaction is a viable alternative of regeneration process of adsorbent agents.

Keywords: Regeneration; Biochar; Dye adsorption; Advanced oxidation processes

1. Introduction

Advanced oxidative processes are considered promising technologies involving the in situ production of strong oxidants, mainly the hydroxyl radical (•OH) [1]. This strong oxidant has a high standard potential ($E°$ = 2.80 V) that allows reactions with almost all organic chemicals giving non-selective mineralization to CO_2, H_2O and inorganic ions [2–5]. In particular, Fenton process has gained attention due to the rapid formation of OH radicals in acid medium according to the following chemical reaction:

$$Fe^{2+} + H_2O_2 \rightarrow + Fe^3 + HO^{\bullet} + HO^- \quad (1)$$

The efficiency of the Fenton reaction in the degradation of textile dyes in aqueous solutions is well known in the literature [6–16]. Some works suggested Fenton reaction to remediate loaded adsorbents [17–20]. However, few studies

* Corresponding author.

have analyzed the application of advanced oxidative process in this direction is the present work aims to evaluate the efficiency of the Fenton reaction to degrade the dye methylene blue adsorbed on a biochar surface. *Syagrus coronata* biomass was used as raw material for the production of the biochar. The licuri or ouricuri (*Syagrus coronata* (Mart) Becc.) is one of the main native palm trees of the Brazilian semi-arid. In this region, it has the capacity to withstand prolonged droughts, blooming and fruiting for a long period of the year. It is used in animal feeding (caprine and poultry farming), human food, handicraft production, wax production, civil construction, cosmetics industry, soap-making and paint manufacture, as well as having a high potential for ornamental purposes and for the production of biodiesel. The endocarp, one of the layers that make up the fruit, is used in the manufacture of handicrafts [21–28]. However, the amount of raw material generated is larger than the one used in commercial applications and it is often discarded, causing an environmental problem. Therefore, it is important to investigate alternative applications of this biomass. In particular, this study proposes the biochar production from the ouricuri endocarp to reduce the environmental impact and use it as an adsorbent in water treatment.

In summary, this paper reports the application of the ouricuri endocarp biochar for the removal of the methylene blue from aqueous solution and the Fenton reaction as a process to regenerate and recover the adsorbent.

2. Material and methods

2.1. Adsorbent

The biochar used as adsorbent was obtained from the ouricuri (*Syagrus coronata*) endocarp pyrolysis. The cassava strain was cut into smaller pieces of different sizes. Pyrolysis was carried out in a pyrolysis unit, the sample was inserted in the cylindrical vertical reactor (D = 70 mm, H = 370 mm). The reactor was made of carbon steel. A heating system, tube furnace (Jung/LT6 2010) with temperature control system was used to provide the required temperature. The gases (condensables and not condensables) formed in the pyrolysis were suctioned by a vacuum pump (FANEM/089-Cal, maximum volumetric flow rate of 0.024 m^3 min^{-1} and power rating of 550 W) at 100 mmHg. A thermostatic bath (TECNAL/TE184) allowed the circulation of water in two series columns of condensation with 2 Allihn condensers each, where the condensable volatiles were obtained. The pyrolitic oils were collected and stored in kitassatos. The conditions used for pyrolysis of cassava stump were as follows: initial temperature of 30°C; final temperatures of 400°C and 800°C; heating rate of 20°C min^{-1} and residence time of 2 h. The adsorbent was washed, ground and separated for its further use in dye adsorption and regeneration studies.

2.2. Experimental design for testing the dye adsorption

A 2^3 factorial experimental design was carried out to evaluate the influence of adsorbent mass m (2.4 and 4.8 g), particle diameter D (<0.149 and average particle diameter of 0.993 mm) and pyrolysis temperature T (400°C and 800°C) on the dye adsorption in order to determine the best working conditions. Experimental tests were performed in random order and replicate to guarantee the reproducibility of the experimental data resulting in 8 adsorption experiments. The variable response used to determine the efficicacy of the adsorption process was the dye adsorption capacity (q_t, mg g^{-1}). Batch adsorption tests were performed with 250 mL beakers containing 60 mL of the 100 mg L^{-1} dye solution. These experiments were carried out at 27°C ± 2°C, without pH adjustment and 500 rpm using a magnetic stirrer (SPLABOR SP-10003/S) with a contact time adsorbent – dye solution of 180 min and the samples were centrifuged at the end of each test. Dye concentrations were quantified by UV-Visible spectrometer (SHIMADZU multipesc-1501, Japan) at the maximum absorbance wavelength of the methylene blue dye (665 nm) [27,29]. The amount of dye adsorbed per mass of adsorbent at equilibrium was calculated using Eq. (2)

$$q_t = \frac{C_0 - C_f}{m} \times V \tag{2}$$

where C_0 is the initial dye concentration used in adsorption test (mg L^{-1}), C_f is the final dye concentration in the adsorption test (mg L^{-1}) and V is the solution volume (L). Biochar obtained with the best experimental condition from the factorial design was characterized and used in dye adsorption kinetic and equilibrium studies and Fenton regeneration.

2.3. Adsorbent characterization

The characterization of the biochar was performed using thermal gravimetry (TG)/derivative thermal gravimetry (DTG) analysis and X-ray diffraction (XRD). Thermal analyzes were performed on a Shimadzu-TG-50 (Japan) equipment in the range of 25°C–900°C. XRD patterns of the biochar were obtained with a Cu-Ka source, which operated at a voltage of 40 KV with 30 mA of current using a Shimadzu XRD-6000 diffractometer (Japan). These characterization analyzes were performed for the adsorbent before contact with the dye solution.

2.4. Dye kinetic studies

Samples were collected to obtain the kinetic curve at the pre-defined times of 0, 5, 10, 15, 30, 60, 120 and 180 min, without pH adjustment, at 27°C ± 2°C for different dye concentrations (50, 100 and 200 mg L^{-1}) with magnetic stirring of 500 rpm. In this study, the pseudo-first-order (PFO) and pseudo-second-order (PSO) kinetic models were applied. [29–32] expressed in Eqs. (3) and (4).

$$q_t = q_e\left(1 - e^{-k_1 \times t}\right) \tag{3}$$

$$q_t = \frac{k_2 \times t \times q_e^2}{\left(1 + k_2 \times t \times q_e\right)} \tag{4}$$

where k_1 and k_2 are first and second order adsorption kinetics (min^{-1} and g mg^{-1} h^{-1}) respectively, q_t and q_e are the adsorbed adsorbent (mg g^{-1}) in time respectively.

2.5. Dye equilibrium studies

Adsorption isotherms were performed for dye solutions with concentrations of 25, 50, 100, 150, 200 and 300 mg L^{-1}, without pH adjustment, at 27°C ± 2°C. Heterogeneous system adsorbent-dye solution was kept under constant stirring (500 rpm) for 180 min, as determined by kinetics. After this period, the samples were centrifuged and the dye concentration was quantified. For adsorption equilibrium modeling, Langmuir [33], Freundlich [34], Sips [35] and Redlich–Peterson [36] were used, according to Eqs. (5)–(8), respectively.

$$q_e = \frac{q_{\max} \times K_L \times C_e}{1 + K_L \times C_e} \tag{5}$$

$$q_e = K_F C_e^{1/n} \tag{6}$$

$$q_e = \frac{q_{\max} \times K_S \times C_e^{m_s}}{1 + K_s \times C_e^{m_s}} \tag{7}$$

$$q_e = \frac{K_R \times C_e}{1 + a_R \times C_e^{\beta}} \tag{8}$$

where $q_{\max}$ represents the maximum adsorption capacity (mg g^{-1}), K_L is the adsorption equilibrium constant that is usually related to the affinity between adsorbent and adsorbate (L g^{-1}), K_F and n are Freundlich parameters, K_S is the equilibrium constant of the Sips model (L mg^{-1}), m_S is the exponent of the Sips model, K_R is the Redlich–Peterson isotherm model constant (L mg^{-1}), a_R is the Redlich–Peterson isotherm constant (L mg^{-1}) and β is the Redlich–Peterson isotherm model exponent, respectively. Parameters of all isotherm models were determined with a nonlinear regression approach.

2.6. Fenton reactions for the biochar regeneration

This study was carried out to analyze the influence of the Fenton reagents on the biochar regeneration efficiency and the advantageous of a hybrid adsorption/oxidation process for methylene blue removal. Before initiating the regeneration tests, the saturation of the biochar was carried out with 60 mL of methylene blue dye solution at 300 mg L^{-1} and using different contact times (0, 5, 10, 15 and 30 min) under constant stirring at 27°C ± 2°C and without pH adjustment. Dye-loaded biochar was mixed with 50 mL of distilled water at 27°C ± 2°C under constant stirring of 500 rpm. pH of the adsorbent-water system was adjusted to 3.0 and the Fenton reagents were added at different concentrations of Fe^{2+} (0.5–1.0 mmol L^{-1}) and H_2O_2 (100–2,400 mmol L^{-1}). The reaction time was 30 min for these regeneration studies. Biochar was separated from the solution and rinsed with distilled water. This adsorbent was used to carry out the next adsorption cycle under the same operating conditions to verify the efficiency of the Fenton process in the regeneration of the biochar. The concentration of the dye in the solution was determined by UV-Visible spectrophotometry.

3. Results

3.1. Experimental design

The evaluation of 2^3 factorial design revealed that the endocarp of ouricuri can retain the methylene blue dye. The calculations of the effects of the variables and the interactions between them showed that the most influential variable in the adsorption process was the mass of the adsorbent, followed by the particle diameter and the interaction effects of the adsorbent and particle diameter. These results are shown in the Pareto diagram in Fig. 1.

The mass effect was positive, that is, the highest value of the adsorption capacity was obtained for the highest mass level. By decreasing the mass of the adsorbent from 4.8 to 2.4 g, there was a mean decrease in the removal capacity of 43%. Therefore, it can be concluded that the highest amount of adsorbed dye is reached when the mass effect is at its upper level, for the range studied in this experimental design. The response surfaces for the interactions of two factors that were statistically significant are shown in Fig. 2.

As depicted in Fig. 2a, the highest removal capacity was obtained for the smaller particle diameter and higher mass of the adsorbent. Fig. 2b shows that the best removal capacity results can be obtained for the higher pyrolysis temperature and lower particle diameter. Besinella Junior et al. [37] also evaluated the effect of the coconut shell particles sizes used to produce activated carbon for the adsorption of the reactant dye Remazol Golden Yellow RNL. It was observed a greater adsorption capacity for samples of smaller size, which could be explained by the increase of the superficial area of particles that are in contact with the fluid phase. The efficiency increase as a function of the pyrolysis temperature is also associated to the increment of the surface area of the biochar [38]. The highest percentage of adsorbed dye removal was 99.4%, obtained with 4.8 g of adsorbent, 800°C as pyrolysis temperature and particle diameter <0.149 mm.

From the data achieved by the linear regression, an empirical model was obtained to predict the removal capacity of methylene blue by the ouricuri endocarp biochar (Eq. (9)):

$$\text{Removal \%} = 76.92 + 19.44x_M - 4.93x_D + 3.59x_{\text{MD}} + 1.22x_{\text{MT}} + 1.72x_{\text{DT}} - 2.17x_{\text{MD}} \tag{9}$$

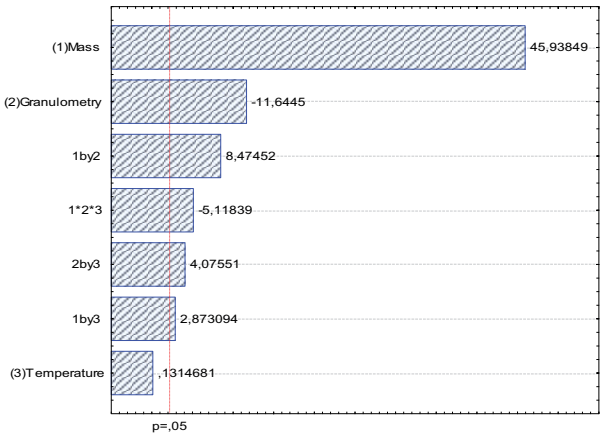

Fig. 1. Pareto diagram.

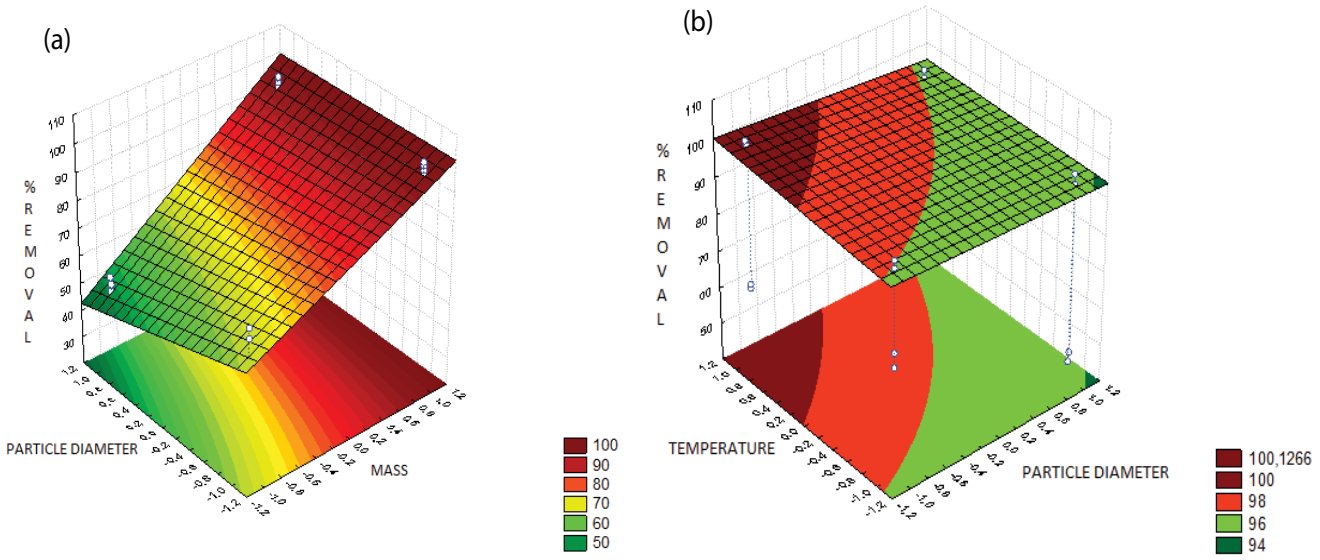

Fig. 2. Response surfaces for % of removal: (a) adsorbent mass vs. particle diameter and (b) particle diameter vs. pyrolysis temperature.

where x_M = mass; x_D = diameter; x_{MD} = mass vs. diameter; x_{MT} = mass vs. temperature; x_{DT} = diameter vs. temperature; x_{MDT} = mass vs. diameter vs. temperature, encoded.

Table 1 shows the analysis of variance for the linear model proposed to explain the response of the removal capacity according to the studied parameters. Considering the data presented in Table 1, the regression is significant to describe the experimental results and the linear model can be used to predict the behavior of the process. For 95% of confidence interval, the calculated F (F_{calc}) was 102.75, greater than the tabulated F value (F_{tab}) of 3.37, then the model can be used to estimate the removal capacity efficiency in relation to the evaluated parameters. In addition to the result of the F test, it can be seen in Table 1 that the correlation coefficient (R^2) was equal to 0.99, close to unity, and that all main effects and interactions were significant, indicating that the model was well adjusted to the experimental data.

3.2. Adsorbent characterization

Fig. 3a and b shows the X-ray diffractogram for the biochar produced at 800°C. This technique can be applied to evaluate the crystallinity and structure of the biochar, consisting of a powerful identification tool for the samples. The diffractogram shows two peasks around 22°, characteristic of Cellulose type I, which suggests that the crystalline structure of the cellulose was not altered during the production. The crystalline arrangements in the cellulose appear due to the formation of inter- and intramolecular H-bonding by the hydroxyl groups. H-bonding restricts the free movement of the cellulosic chains, which align with each other in an ordered manner, which tends to have crystallinity [39,40]. It is possible to observe in Fig. 3b that the material did not show the presence of the dyestuff. It is possible to infer that the dye disappeared and the integrity of the material was maintained [19]. Then, the decrease in the efficiency (see section 3.4) could be related to the competition of the active sites by the resultant ions from Fenton reactants, hampering the dye access to these sites.

The thermogravimetric analysis (TGA) aimed to obtain information about the structure stability of the adsorbent material. The biochar TG curve is shown in Fig. 4. The biochar thermogram showed a mass loss from room temperature (25°C) to approximately 100°C due to the loss of water from the material. Between 150°C to approximately 500°C, the mass loss becomes linear. The material presented a relative thermal stability. The second mass loss corresponds to the degradation of volatile products derived from lignin, including phenolics, alcohols, acids, aldehydes, along with the formation of gaseous products being removed [41]. It can also be verified by the TGA that at the temperature of approximately 500°C is related to the release of volatile compounds, constituted by oxygen and

Table 1
Analysis of variance (ANOVA)

Source of variation	Sum of the squares (SQ)	Degrees of freedom	Mean of the squares (MQ)
Regression	6,710.04	6	1,118.34
Residues	97.95	9	10.88
Total	6,807.99	15	–
R^2	0.99	–	–

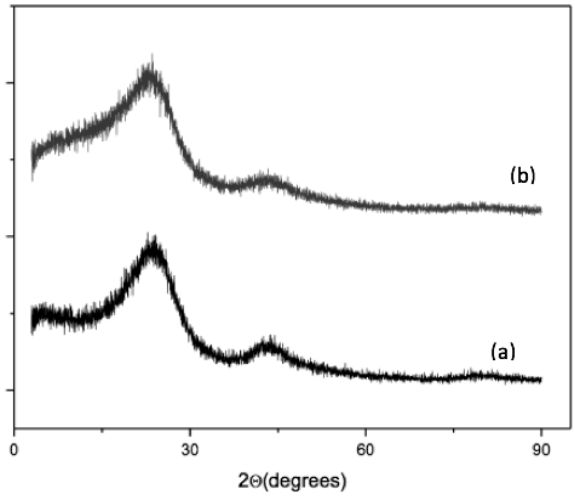

Fig. 3. XRD for biochar (a) produced at 800°C and (b) regenerated by Fenton (Fe^{2+} 1.0 mmol L^{-1} and H_2O_2 600 mmol L^{-1}).

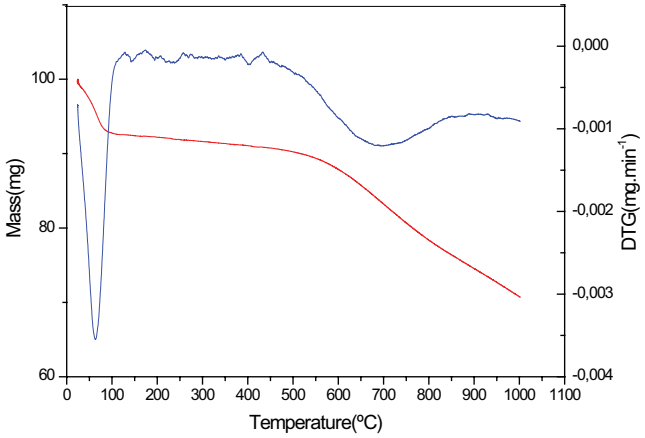

Fig. 4. Thermogravimetry analysis of biochar produced at 800°C: (—) TGA and (—) DTG.

hydrogen, as the remaining carboxyl compounds of the pyrolysis process [42].

3.3. Adsorption studies

The kinetic study plays an important role when using an adsorbent to treat effluents, since it is possible to define the equilibrium time and the velocity of the adsorption process. Therefore, it is necessary to evaluate models that can describe and predict the behavior of the studied process. The kinetic evolution of the methylene blue dye adsorption using the ouricuri endocarp biochar in shown in Fig. 5.

The kinetics were rapid in the first 5 min and after 60 min the equilibrium occurred. According to Wang and Zhu, the adsorption of dyes is fast at the initial contact time and then slows down and stagnates with increasing contact time. The high adsorption capacity of the methylene blue dye in the first instants of the assay was already reported by Al-Ghouti et al. [44] and Deng et al. [45], which justifies this fact with the presence of acidic functional groups found

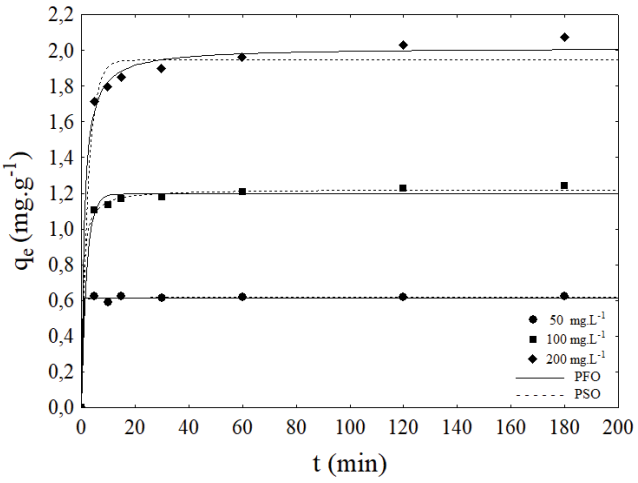

Fig. 5. Kinetic evaluation of adsorption of methylene blue onto ouricuri endocarp biochar. C_0 = 50, 100 and 150 mg L^{-1}, T = 800°C, D = <0.149 mm and M = 4.8 g for 60 mL of solution.

on the surface of the adsorbent, and which have a certain affinity with the methylene blue molecules. Thus, it is likely that the adsorption of the dye has occurred first on the surface and then, through diffusion into the sites present in the adsorbent material, becoming slower.

The results obtained are shown in Table 2. The pseudo-second-order model presented the best fit with R^2 correlation coefficient equal to 0.99, a mean value of k_2 of 1.09 g mg^{-1} min^{-1} and a calculated value of 1.23 mg g^{-1}. The value of q_e calculated by the model was close to the experimental data, 1.20 mg g^{-1}, as expected for a well-adjusted model.

Considering the correlation coefficients obtained in each equation, as well as the values of q and estimated from these equations, the most appropriated mechanism to the obtained experimental values refers to the one of pseudo-second-order, which describes the involvement of two consecutive steps in the process of adsorption: external diffusion and diffusion through the pores of the solid [46].

The result of the adsorption isotherm of the methylene blue dye on the biochar is shown in Fig. 6. The adsorption capacity increases according to the equilibrium concentration of the dye in the medium until it reaches a complete saturation of the surface at higher concentrations. The isotherms can often be represented by theoretical models, with Langmuir, Freundlich, Sips and Redlich–Peterson models being the most used. The adsorption isotherm model describes how the adsorbate interacts with the adsorbent allowing to find the most efficient application of the adsorbent. In this particular case, the experimental results were more consistent with the Sips model. These results are summarized in Table 3 and the application of the models are depicted in Fig. 6.

The models were compared using the R^2 value as reference. The results of Table 3 show that both Sips and Langmuir models represent well the experimental data obtained in this study. However, with the evaluation of the average relative error, ARE, the Sips model presented a smaller value of the error function, indicating that this model was better fitted to the experimental data. It is also observed,

Table 2
Kinetic parameters

Model	50 mg L^{-1}	100 mg L^{-1}	200 mg L^{-1}
$q_{experimental}$	0.6225	1.2438	2.0738
PFO			
q_1 (mg g^{-1})	0.6152	1.1955	1.9454
k_1 (min^{-1})	5.7873	0.4961	0.3954
R^2	0.9967	0.9934	0.9851
ARE (%)	1.48	2.37	3.86
PSO			
q_2 (mg g^{-1})	0.6169	1.2230	2.0149
k_2 (min^{-1})	37.5993	1.3269	0.4781
R^2	0.9970	0.9985	0.9959
ARE (%)	1.46	1.23	2.16

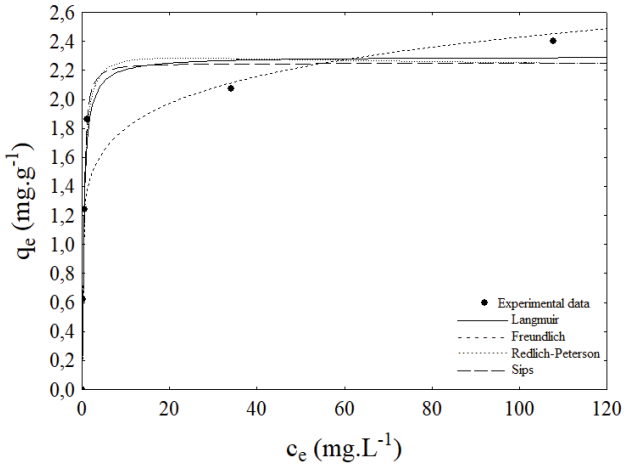

Fig. 6. Isotherm of adsorption of methylene blue onto ouricuri endocarp biochar with equilibrium models fits. T = 800°C, D = <0.149 mm and M = 4.8 g for 60 mL of solution.

in Table 3, that the function adsorption error decreases in the order Sips > Langmuir > Redlich–Peterson > Freundlich for the dye studied.

Sips model combines elements of the Langmuir and Freundlich equations and predicts that at low concentrations of adsorbate, it reduces the Freundlich isotherm, while at high concentrations, the Langmuir isotherm is reduced, characterizing a monolayer adsorption [47]. From the economic point of view, these results are highly satisfactory. Moreover, a short time is required for the process to be fully effective (kinetic results can prove this).

3.4. Regeneration study

The results obtained for the biocarbon regeneration study are shown in Fig. 7. The untreated biocarbon is saturated and in its reuse a reduction of only 7% of the dye concentration was obtained. After the Fenton reaction, it was observed that the iron concentration has negligenciable

Table 3
Isotherm parameters for the adsorption of methylene blue onto ouricuri endocarp biochar

Models	Parameters	27°C ± 2°C
Langmuir	q_{max} (mg g^{-1})	2.2956
	K_L (L mg^{-1})	2.4578
	R^2	0.9768
	ARE (%)	9.11
Freundlich	N	7.7253
	K_F ([mg L^{-1}][L g^{-1}]$^{-1/n}$)	1.3382
	R^2	0.8894
	ARE (%)	21.39
Redlich–Peterson	K_R	5.1131
	a_R (L mg^{-1})$^{\beta}$	2.0641
	B	1.0196
	R^2	0.9778
	ARE (%)	8.25
Sips	q_{max} (mg g^{-1})	2.2482
	K_s (L mg^{-1})	3.5989
	m_S	1.4125
	R^2	0.9865
	ARE (%)	4.84

influence on the efficiency of the Fenton reaction in the regeneration of the biochar. From the Fenton conditions in which the Fe^{2+} concentration was fixed at 1.0 mmol L^{-1} and the concentration of H_2O_2 was increased to 600 mmol L^{-1}, the highest regeneration efficiency, 19.31%, was obtained. However, when the concentration of H_2O_2 was increased to 1,200 and 2,400 mmol L^{-1}, there was a decrease in the adsorption capacity of the biochar, indicating that the excess of H_2O_2 decreases the regeneration efficiency.

Therefore, a positive effect on dye removal was expected by increasing the concentrations of Fenton reagents. However, it was observed that an excess of H_2O_2 may prejudice the performance of the process, since these species can subsequently react with the hydroxyl radical (Eqs. (10)–(12)), resulting in a competition with the organic compounds to be degraded [48]. With the excess of hydroxyl radical, the radicals can react with each other (Eq. (13)) and decrease the efficiency of the process.

$$HO + Fe^{2+} \rightarrow Fe^{3+} + OH^- \qquad k_5 = 4.3\times10^8\ M^{-1}\ s^{-1} \qquad (10)$$

$$HO^{\bullet} + H_2O_2 \rightarrow HO_2^{\bullet} + H_2O \qquad k_4 = \left(1.2-4.5\right)\times10^7 M^{-1}s^{-1} \qquad (11)$$

$$HO^{\bullet} + HO_2^{\bullet} \rightarrow O_2 + H_2O \qquad k_7 = 1\times10^{10}\ M^{-1}s^{-1} \qquad (12)$$

$$HO^{\bullet} + {}^{\bullet}OH \rightarrow H_2O_2 \qquad k_6 = 5.3\times10^9 M^{-1}s^{-1} \qquad (13)$$

Removal efficiency after the Fenton treatment increased in the initial 5 min, probably due to the desorption of both

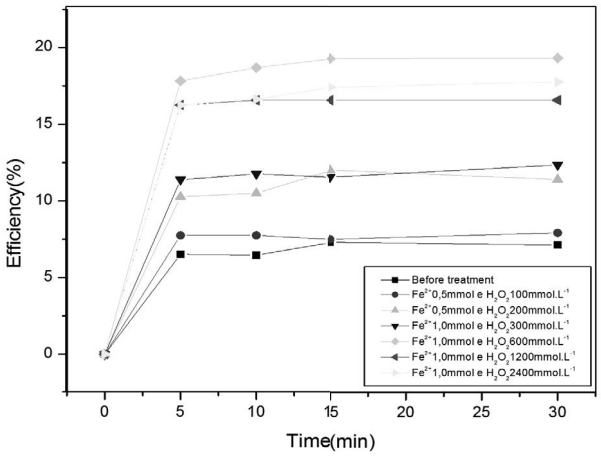

Fig. 7. Regeneration of ouricuri endocarp biochar saturated with methylene blue dye.

the dye and the oxidation intermediates during the reaction, and after that reaction time, it slowed down and stagnated when increasing the contact time. The decrease in the efficiency of the combined adsorption–Fenton regeneration process could suggests that an interaction occurs between the methylene blue dye and the oxygen groups present on the surface of the biochar through a chemical adsorption mechanism, making dye desorption difficult.

4. Conclusions

From the results of experimental design, it was possible to analyze that the variable of greater influence in the adsorption process was the mass of the adsorbent, followed by the particle diameter. The best conditions to obtain the maximum removal capacity of the methylene blue dye were the adsorbent mass of 4.8 g, the pyrolysis temperature of 800°C and the particle diameter <0.149 mm, conditions used in the kinetic study of balance and regeneration.

The kinetic behavior showed that the adsorption was very fast in the first 5 min and the equilibrium was reached after 60 min; The pseudo-second-order model presented the best fit, demonstrating that the adsorption mechanism occurs in two steps, an external diffusion and a diffusion through the pores of the solid. The equilibrium studies indicated a favorable adsorption behavior and the Sips model had the best fit with the experimental data. In the regeneration study, it was observed a good recovery of the adsorption capacity. The best regeneration conditions were obtained with the Fenton reagents: Fe^{2+} 1.0 mmol L^{-1} and H_2O_2 600 mmol L^{-1}.

In brief, it is possible to conclude that the biochar obtained by the pyrolysis of the *Syagrus coronata* endocarp is a great adsorbent to remove methylene blue from aqueous media. Moreover, In addition, the use of ouricuri as a source of biomass for the biochar production consists of an alternative application of this agricultural residue. Regarding the desorption of the saturated adsorbent, Fenton reaction can be a viable, simple and low-cost alternative used for the regeneration process.

Acknowledgments

The authors thank the Conselho Nacional de Desenvolvimento Científico e Tecnológico (CNPq/Brazil), Coordenaçao de Aperfeiçoamento de Pessoal de Nível Superior (CAPES/Brazil) and Fundação de Amparo à Pesquisa do Estado de Alagoas (FAPEAL/Brazil).

References

[1] M.A. Oturan, J.-J. Aaron, Advanced oxidation processes in water/wastewater treatment: principles and applications. A review, Crit. Rev. Env. Sci. Technol., 44 (2014) 2577–2641.
[2] C.A. Martínez-Huitle, E. Brillas, Decontamination of wastewaters containing synthetic organic dyes by electrochemical methods: a general review, Appl. Catal., B, 87 (2009) 105–145.
[3] E. Brillas, I. Sirés, M.A. Oturan, Electro-Fenton process and related electrochemical technologies based on Fenton's reaction chemistry, Chem. Rev., 109 (2009) 6570–6631.
[4] I. Sirés, E. Brillas, M.A. Oturan, M.A. Rodrigo, M. Panizza, Electrochemical advanced oxidation processes: today and tomorrow. A review, Environ. Sci. Pollut. Res., 21 (2014) 8336–8367.
[5] M.A. Rodrigo, M.A. Oturan, N. Oturan, Electrochemically assisted remediation of pesticides in soils and water: a review, Chem. Rev., 114 (2014) 8720–8745.
[6] R. Liu, H.M. Chiu, C.-S. Shiau, R.Y.-L. Yeh, Y.-T. Hung, Degradation and sludge production of textile dyes by Fenton and photo-Fenton processes, Dyes Pigm., 73 (2007) 1–6.
[7] H. Fida, G. Zhang, S. Guo, A. Naeem, Heterogeneous Fenton degradation of organic dyes in batch and fixed bed using La-Fe montmorillonite as catalyst, J. Colloid Interface Sci., 490 (2017) 859–868.
[8] M.R. Sohrabi, A. Khavaran, S. Shariati, S. Shariati, Removal of Carmoisine edible dye by Fenton and photo Fenton processes using Taguchi orthogonal array design, Arabian J. Chem., 10 (2017) S3523–S3531.
[9] N.C. Fernandes, L.B. Brito, G.G. Costa, S.F. Taveira, M.S.S. Cunha–Filho, G.A.R. Oliveira, R.N. Marreto, Removal of azo dye using Fenton and Fenton-like processes: evaluation of process factors by Box–Behnken design and ecotoxicity tests, Chem. Biol. Interact., 291 (2018) 47–54.
[10] X. Xue, K. Hanna, N. Deng, Fenton-like oxidation of Rhodamine B in the presence of two types of iron (II, III) oxide, J. Hazard. Mater., 166 (2009) 407–414.
[11] X. Liu, M. Qiu, C. Huang, Degradation of the Reactive Black 5 by Fenton and Fenton-like system, Procedia Eng., 15 (2011) 4835–4840.
[12] H.-J. Fan, S.-T. Huang, W.-H. Chung, J.-L. Jan, W.-Y. Lin, C.-C. Chen, Degradation pathways of crystal violet by Fenton and Fenton-like systems: condition optimization and intermediate separation and identification, J. Hazard. Mater., 171 (2009) 1032–1044.
[13] F. Martínez, P. Leo, G. Orcajo, M. Díaz-García, M. Sanchez-Sanchez, G. Calleja, Sustainable Fe-BTC catalyst for efficient removal of mehylene blue by advanced Fenton oxidation, Catal. Today, 313 (2018) 6–11.
[14] X.-R. Xu, H.-B. Li, W.-H. Wang, J.-D. Gu, Degradation of dyes in aqueous solutions by the Fenton process, Chemosphere, 57 (2004) 595–600.
[15] S. Wang, A Comparative study of Fenton and Fenton-like reaction kinetics in decolourisation of wastewater, Dyes Pigm., 76 (2008) 714–720.
[16] A.M.S. Solano, S. Garcia-Segura, C.A. Martínez-Huitle, E. Brillas, Degradation of acidic aqueous solutions of the diazo dye Congo Red by photo-assisted electrochemical processes based on Fenton's reaction chemistry, Appl. Catal., B, 168–169 (2015) 559–571.
[17] A.P. Díaz Gómez-Treviño, V. Martínez-Miranda, M. Solache-Ríos, Removal of remazol yellow from aqueous solutions by unmodified and stabilized iron modified clay, Appl. Clay Sci., 80–81 (2013) 219–225.

[18] P.T. Almazán-Sánchez, M.J. Solache-Ríos, I. Linares-Hernández, V. Martínez-Miranda, Adsorption-regeneration by heterogeneous Fenton process using modified carbon and clay materials for removal of indigo blue, Environ. Technol., 37 (2016) 1843–1856.
[19] E. Rosales, D. Anasie, M. Pazos, I. Lazar, M.A. Sanromán, Kaolinite adsorption-regeneration system for dyestuff treatment by Fenton based processes, Sci. Total Environ., 622–623 (2018) 556–562.
[20] A.M. Díez, M.A. Sanromán, M. Pazos, Fenton-based processes for the regeneration of catalytic adsorbents, Catal. Today, 313 (2018) 122–127.
[21] A.E.B.A. Sousa, Licuri na área de ocorrência da arara-azul-de-lear, C. Lugarini, A.E.A. Barbosa, K.G. Oliveira, Eds., Plano Ação Nac. Para a Conserv. Da Arara-Azul-de-Lear., 2nd ed., Instituto Chico Mendes de Conservação da Biodiversidade - ICMBio, Brasília-Brazil, 2012, pp. 57–76.
[22] M.U. de L. Rufino, J.T. de M. Costa, V.A. da Silva, L. de H.C. Andrade, Conhecimento e uso do ouricuri (*Syagrus coronata*) e do babaçu (Orbignya phalerata) em Buíque, PE, Brasil, Acta Bot. Brasilica, 22 (2008) 1141–1149.
[23] I.C. Crepaldi, L.B. De Almeida-Muradian, M.D.G. Rios, M.D.V.C. Penteado, A. Salatino, Composição nutricional do fruto de licuri (*Syagrus coronata* (Martius) Beccari), Rev. Bras. Botânica., 24 (2001) 155–159.
[24] S. Belviso, D. Ghirardello, M. Giordano, G. Sousa Ribeiro, J. de Souza Alves, S. Parodi, S. Risso, G. Zeppa, Phenolic composition, antioxidant capacity and volatile compounds of licuri (*Syagrus coronata* (Martius) Beccari) fruits as affected by the traditional roasting process, Food Res. Int., 51 (2013) 39–45.
[25] O.K. Iha, F.C.S.C. Alves, P.A.Z. Suarez, M.B.F. de Oliveira, S.M.P. Meneghetti, B.P.T. Santos, J.I. Soletti, Physicochemical properties of *Syagrus coronata* and *Acrocomia aculeata* oils for biofuel production, Ind. Crops Prod., 62 (2014) 318–322.
[26] S.D. Segall, W.E. Artz, D.S. Raslan, V.P. Ferraz, J.A. Takahashi, Ouricuri (*Syagrus coronata*) triacylglycerol analysis using HPLC and positive ion electrospray tandem MS, J. Am. Oil Chem. Soc., 81 (2004) 143–149.
[27] L. Meili, T.S. da Silva, D.C. Henrique, J.I. Soletti, S.H.V. de Carvalho, E.J. da Silva Fonseca, A.R.F. de Almeida, G.L. Dotto, Ouricuri (*Syagrus coronata*) fiber: a novel biosorbent to remove methylene blue from aqueous solutions, Water Sci. Technol., 75 (2017) 106–114.
[28] K. Teixeira da Silva de La Salles, S.M.P. Meneghetti, W. Ferreira de La Salles, M.R. Meneghetti, I.C.F. dos Santos, J.P.V. da Silva, S.H.V. de Carvalho, J.I. Soletti, Characterization of *Syagrus coronata* (Mart.) Becc. oil and properties of methyl esters for use as biodiesel, Ind. Crops Prod., 32 (2010) 518–521.
[29] D.S. Paz, A. Baiotto, M. Schwaab, M.A. Mazutti, M.M. Bassaco, D.A. Bertuol, E.L. Foletto, L. Meili, Use of papaya seeds as a biosorbent of methylene blue from aqueous solution, Water Sci. Technol., 68 (2013) 441–447.
[30] S. Lagergren, About the theory of so-called adsorption of soluble substances, K. Sven. Vetenskapsakad., 24 (1898) 1–39.
[31] Y.S. Ho, G. McKay, Sorption of dye from aqueous solution by peat, Chem. Eng. J., 70 (1998) 115–124.
[32] Y.S. Ho, G. McKay, Pseudo-second order model for sorption processes, Process Biochem., 34 (1999) 451–465.
[33] Y.S. Ho, G. McKay, A comparison of chemisorption kinetic models applied to pollutant removal on various sorbents, Process Saf. Environ. Prot., 76 (1998) 332–340.
[34] I. Langmuir, The adsorption of gases on plane surfaces of glass, mica and platinum, J. Am. Chem. Soc., 40 (1918) 1361–1403.
[35] H. Freundlich, Over the adsorption in solution, J. Phys. Chem., 57 (1906) 358–471.
[36] R. Sips, On the structure of a catalyst surface, J. Phys. Chem., 16 (1948) 490–495.
[37] O. Redlich, D.L. Peterson, A useful adsorption isotherm, J. Phys. Chem., 63 (1959) 1024.
[38] E. Besinella Junior, M.S. Matsuo, M. Walz, A.F. da Silva, C.F. da Silva, Effects of temperature and particle size on the adsorption of remazol golden yellow rnl in activated carbon, Acta Sci. Technol., 31 (2009) 185–193.
[39] J. Tang, W. Zhu, R. Kookana, A. Katayama, Characteristics of biochar and its application in remediation of contaminated soil, J. Biosci. Bioeng., 116 (2013) 653–659.
[40] D. Watkins, M. Nuruddin, M. Hosur, A. Tcherbi-Narteh, S. Jeelani, Extraction and characterization of lignin from different biomass resources, J. Mater. Res. Technol. 4 (2015) 26–32.
[41] M.A.A. Zaini, M. Zakaria, S.H. Mohd.-Setapar, M.A. Che-Yunus, Sludge-adsorbents from palm oil mill effluent for methylene blue removal, J. Environ. Chem. Eng., 1 (2013) 1091–1098.
[42] C.J. Chirayil, J. Joy, L. Mathew, M. Mozetic, J. Koetz, S. Thomas, Isolation and characterization of cellulose nanofibrils from *Helicteres isora* plant, Ind. Crops Prod., 59 (2014) 27–34.
[43] Y. Nishiyama, Structure and properties of the cellulose microfibril, J. Wood Sci., 55 (2009) 241–249.
[44] M.A. Al-Ghouti, M.A.M. Khraisheh, M.N.M. Ahmad, S. Allen, Adsorption behaviour of methylene blue onto Jordanian diatomite: a kinetic study, J. Hazard. Mater., 165 (2009) 589–598.
[45] H. Deng, J. Lu, G. Li, G. Zhang, X. Wang, Adsorption of methylene blue on adsorbent materials produced from cotton stalk, Chem. Eng. J., 172 (2011) 326–334.
[46] Y.S. Ho, G. Mckay, Kinetic models for the sorption of dye from aqueous solution by wood, Process Saf. Environ. Prot., 76 (1998) 183–191.
[47] O. Hamdaoui, E. Naffrechoux, Modeling of adsorption isotherms of phenol and chlorophenols onto granular activated carbon: part II. Models with more than two parameters, J. Hazard. Mater., 147 (2007) 401–411.
[48] R. Maciel, G.L. Sant'Anna Jr., M. Dezotti, Phenol removal from high salinity effluents using Fenton's reagent and photo-Fenton reactions, Chemosphere, 57 (2004) 711–719.